

Experimental evidence of the atmospheric convective transport contribution to sessile droplet evaporation

F. Carle,^{1,a)} B. Sobac,^{1,2} and D. Brutin^{1,b)}

¹IUSTI Laboratory, UMR 7343 CNRS, Aix-Marseille University, 5 rue Enrico Fermi, 13453 Marseille cedex 13, France

²Transfers, Interfaces and Processes (TIPs), Université Libre de Bruxelles, Brussels, Belgium

(Received 17 December 2012; accepted 30 January 2013; published online 14 February 2013)

We investigate the contribution of the natural convective transport in the vapor phase on the evaporation rate of an evaporating sessile droplet. When comparing the experimental data with the quasi-steady diffusion-controlled evaporation model, an increasing deviation with substrate temperature that was attributed to the effect of the natural convection on the vapor field has been recently highlighted. To validate this analysis, we present experimental results obtained with two gravity levels: 1 *g* and μ *g*. The contribution of the natural convection is analyzed with the Grashof number, and an empirical model is developed combining diffusive and convective transport. © 2013 American Institute of Physics. [<http://dx.doi.org/10.1063/1.4792058>]

The fundamental phenomenon of the evaporation of sessile droplets, despite the vast number of studies and publications devoted to it for almost half a century, is still a field that attracts a high level of interest due to its wide applicability and its complexity. Drying droplets are influenced by several factors: those inherent to the fluid composition (pure liquid,^{1,2} solution of particles,^{3–5} or polymers⁶), those inherent to the support (substrate properties from roughness and wetting^{7–10} to thermal properties^{11–14}), and those depending on the environmental conditions (non-heated^{1–3} or heated substrates,^{14–16} air flow,¹⁷ or humidity¹⁸). Having a better understanding of evaporation is of capital interest to have more control over the various applications, e.g., printing and coating technologies, spray cooling, biochemical assays, deposition of DNA/RNA micro-arrays, and the manufacture of novel optical and electronic materials.

Most research in the last decade dealt with the evaporation kinetics and resulted in models predicting the evaporation rate of sessile droplets. The classical description considers the evaporation as a quasi-steady process controlled by the diffusion of vapor into the air, and the whole system is being assumed to be isothermal at the ambient temperature.^{2,3,19} This model well-describes experimental results whatever the wettability and the volume of spherical droplets evaporating at ambient temperature.^{9,10} However, the descriptive ability of this model begins to be questioned as soon as the thermal effects related to evaporation are no longer negligible, i.e., when the substrate is a thermal insulator^{11,13,14} or when the substrate temperature increases.^{14,16} Indeed, in the last case, the isothermal diffusion-driven model underpredicts the evaporation rate, and a deviation between experiments and the model develops and increases with the substrate temperature as shown in Figure 1 (top).

In this letter, we experimentally highlight, thanks to experiments performed at two gravity levels, that the isothermal diffusion-controlled model correctly describes the evaporation in the absence of gravity, validating the assumptions

inherent in this model. The deviation that develops as the substrate temperature increases at normal gravity is consequently due only to the effect of the buoyant natural convection transport on the vapor phase, which significantly increases the evaporation rate. The contribution of the thermal or solutal effects on convection is analyzed, and the purely diffusive model is empirically extended to a more global model, taking into account the diffusive and convective transport in the gas phase.

Two sets of experiments were conducted with similar setups under terrestrial (1 *g*) and reduced gravity (μ *g*) conditions (performed with parabolic flights). Ethanol droplets were evaporated in air at the temperature of 25 °C onto a cylindrical heated aluminum substrate (10 mm × 10 mm) coated with a Nuflon layer, inside a cell that was large enough to ensure a constant vapor concentration far from the droplet and below saturation to prevent potential external perturbations. The substrate was instrumented by a heat-flux meter that enabled the determination of the evaporation rate ($-dm/dt = Q \cdot S / L_v$, where Q is the heat-flux absorbed by the droplet on the substrate to evaporate, S is the area of the wetting surface, and L_v is the latent heat of vaporization). A high-definition camera was used to laterally visualize and measure the geometrical parameters of the droplets, i.e., base radius R , height h , and contact angle θ . The encountered base radius was always below the capillary length ($l_c = 1.69$ mm in 1 *g* and $l_c = 7.46$ mm in μ *g*); therefore, the droplets had a spherical cap shape. They evaporated in a wetting situation ($\theta_i = 30^\circ$ in 1 *g* and $\theta_i = 23^\circ$ in μ *g*), and the contact line was pinned nearly throughout the entire duration of the evaporation due to the relative importance of the surface roughness ($r_{RMS} = 1.75 \mu\text{m}$). More information about the experimental set-up can be found in Ref. 20.

Figure 1 shows the global evaporation rate plotted as a function of the difference in temperatures of the substrate (T_s) and the ambient air (T_a) for both gravity levels. Each datum point is the evaporation rate given by one single droplet. The uncertainty of the measurements for “1 *g*” and “ μ *g*” has been calculated by the quadratic sum of the absolute uncertainties of each parameters (heat flux, area of wetting, latent

^{a)}Electronic mail: florian.carle@polytech.univ-mrs.fr.

^{b)}Electronic mail: david.brutin@univ-amu.fr.

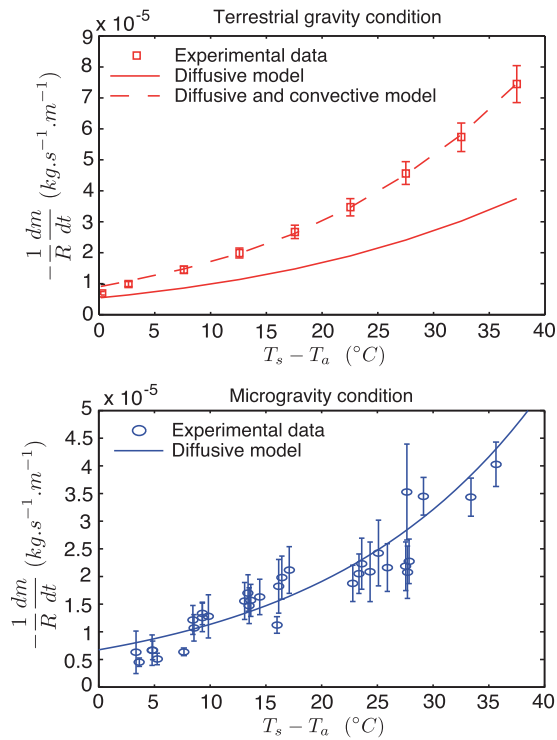


FIG. 1. Evaporation rate by unit length of an ethanol sessile droplet as a function of the temperature difference between the substrate and the ambient air for 1 g (top) and μg conditions (bottom). Information about the power law fits: $-1/R|dm/dt|_{\text{expt}} = a(T_s - T_a)^b$ with $a = 1.36 \times 10^{-9} \text{ kg s}^{-1} \text{ m}^{-1} \text{ K}^{-1}$, $b = 2.62$ (1 g) and $a = 8.75 \times 10^{-9} \text{ kg s}^{-1} \text{ m}^{-1} \text{ K}^{-1}$, $b = 2.061$ (μg).

heat). The experiments reveal that whatever the gravity level, the evaporation rate increases with the substrate temperature following a power law trend. These experimental data are compared to the quasi-steady, diffusion-controlled evaporation model^{2,19} (plane line) defined by

$$-\frac{dm}{dt} = \pi R D \Delta c_v f(\theta), \quad (1)$$

where D is the coefficient of vapor diffusion into air²¹ (for ethanol evaporating into air at 25°C , its value is $1.21 \times 10^{-5} \text{ m}^2/\text{s}$ at 1 bar and $1.49 \times 10^{-5} \text{ m}^2/\text{s}$ at 0.835 bar). $f(\theta) = 1.3 + 0.27 \theta^2$ is a function that depends on the contact angle² (valid in the limit of small contact angles, i.e., $\theta < 90^{\circ}$) which can be approximated² as 1.3 in the limit of small contact angles ($\theta < 40^{\circ}$). $\Delta c_v = c_0 - c_{\infty}$ is the vapor concentration difference between the interface, which is assumed to be saturated at the substrate temperature ($c_0 \approx c_v(T_s)$) and considered to be null far from the droplet because of the large characteristic length of the cell compared to the droplet characteristic length ($c_{\infty} \approx 0$). This diffusion-driven evaporation model implemented with the temperature variation assumes the droplet is isothermal at the substrate temperature. The experiments can actually be considered quasi-steady because the diffusion time is smaller than the evaporation time, $t_D/t_F \approx c_0/\rho \approx 10^{-3} - 10^{-4}$. It is worth mentioning that the values of the evaporation rate given by the model differ for the two sets of experiments due to the adjustment of the diffusion coefficient and the saturated vapor with the temperature and the atmospheric pressure (1 bar on earth and 0.835 bar in the aircraft).

Under terrestrial gravity conditions (top), the experimental value approaches the value of the diffusive model as the substrate temperature is reduced, and at the ambient temperature the experimental value is nearly equal to the model value, consistent with other published results.^{3,9,10} However, as soon as the temperature of the substrate is different from the ambient temperature, the evaporation rate becomes greater than the diffusion-controlled rate, and the difference between the two values increases with the substrate temperature. Thus, this model globally underpredicts the experimental evaporation rate. To evidence how the experimental data deviate from the diffusion-controlled evaporation model, a dimensionless evaporation rate number E^* , which corresponds to the ratio of the measured evaporation rate by the computed one, was introduced and plotted versus a dimensionless temperature in Figure 2. As may be observed, the experimental evaporation rate rapidly diverges accordingly to a power law trend, and the deviation reaches almost 100% at $\tilde{T} = 1.8$.

Under reduced gravity conditions (bottom), both Figures 1 and 2 reveal that the diffusion-controlled evaporation model correctly predicts the experimental data, despite the important dispersion of the data due to perturbations caused by the aircraft flight, for example, by vibrations. This good agreement highlights, for the first time to our knowledge, that this model is valid and can account for the variations in the substrate temperature. In the absence of the effects of gravity, the evaporation can then be correctly assumed to be a quasi-steady, diffusion-controlled process, regardless of the substrate temperature, and the isothermal temperature of the droplet. Indeed, the thermal gradient that develops inside an evaporating droplet driven by the latent heat of vaporization appeared to be negligible when the droplet was sufficiently thin and evaporated on a highly thermally conductive substrate.^{10,13,18}

Consequently, the deviation noticed under the 1 g condition can only be due to the development of another mechanism accompanying the evaporation under the influence of gravity; this additional mechanism to the diffusion increased the evaporation rate. The contribution of this mechanism

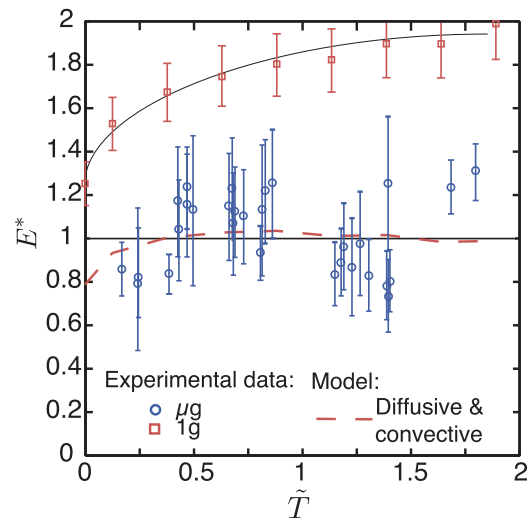


FIG. 2. The dimensionless evaporation rate E^* as a function of the dimensionless temperature $\tilde{T} = (T_s - T_a)/T_a$.

was larger when the substrate temperature was higher. These observations clearly indicate that this mechanism is the natural convection in the vapor phase that develops due to buoyant forces. Because the purely diffusive-controlled evaporation model does not take into account the natural convection, it naturally underestimates the experimental evaporation rate. The natural convection increases the mass transfer in the vapor phase, modifying the vapor field around the droplet by creating a flow motion and renewing the gas around the droplet. This naturally leads to an increase in the evaporation rate as the evaporation is controlled by the difference in the vapor concentration at the interface and at infinity and is generally controlled more by the mass transport in the vapor phase.

Considering that both diffusion and convection are significant in our problem in terrestrial gravity conditions, the evaporation rate can be taken as a sum of a diffusive contribution and a convective contribution:²² $E = E_d + E_c$. The dimensionless evaporation rate is then expressed as $E^* = 1 + E_c^*$, where E_c^* corresponds to the dimensionless evaporation rate due to convection. The deviation from unity observed in Figure 2 shows that the dimensionless contribution of natural convection on the evaporation rate as a function of the temperature. Because convection is induced by buoyancy, we can characterize the convective contribution as a function of the Grashof number Gr , which compares the buoyant forces with the viscous forces (see Figure 3). Natural convection can have two origins in our problem because the system includes both a temperature gradient and a vapor concentration gradient in the gas phase; therefore, we separately considered the two effects and their contributions through the solutal Grashof number, $Gr_s = g\Delta cR^3/\rho\nu^2$ (where g is the gravity acceleration, ν is the kinematic viscosity of air, and Δc is the density difference between the vapor at the droplet interface, c_0 , and the ambient air density, ρ), and the thermal Grashof number, $Gr_t = g\beta\Delta TR^3/\nu^2$ (where $\beta = (1/\rho)(\partial\rho/\partial T) \sim 1/T$ is the coefficient of thermal expansion and $\Delta T = T_s - T_a$).

Figure 3 shows the variation of the convective evaporation term as a function of the Grashof numbers. At ambient temperature, the thermal convection was null because of the absence of a temperature gradient ($Gr_t = 0$). However, a weak solutal convection develops due to the difference in the vapor concentration ($Gr_s = 20.5$). This may explain the

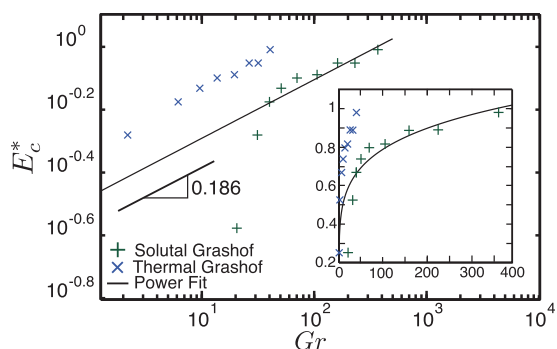


FIG. 3. The variation of the dimensionless convective evaporation term E_c^* as a function of the Grashof number on a log-log scale. The inset shows the same data in Cartesian coordinates.

small deviation in the evaporation rate observed between the experiments and the diffusive model at ambient temperature.²² As soon as the substrate is heated, the thermal convection develops and the convective and solutal convections increase with the temperature. The contribution of the origin of the thermal convection appeared to be weak compared to the origin of the solutal convection because the ratio Gr_t/Gr_s was less than 10% in the range of the investigated temperatures. Thus, we considered as a first approximation that the effect of the thermal convection on the evaporation rate increase was negligible compared to the effect of the solutal convection. Then, as soon as the substrate is heated, the convective evaporation term varies with the Grashof number such that $E_c^* \approx aGr_s^b$, with $a = 0.333 \pm 0.007$ and $b = 0.186 \pm 0.003$ as observed in Figure 3.

By combining the previous equations and employing the ideal gas law, an expression for the evaporation rate that takes into account of the diffusive and naturally convective vapor transport may be derived

$$E = \frac{4RDM_v P_v}{\hat{R}T_s} \left(1 + 0.333 \left[\frac{P_v M_v g}{(P_a - P_v) M_a \nu_a^2} R^3 \right]^{0.186} \right), \quad (2)$$

where M is the molar mass, P is the pressure (considered at saturation as the substrate temperature for the vapor) and the indices a and v specifying the consideration of the air or the vapor, and \hat{R} is the ideal gas constant.

This model was compared to the experimental data in Figures 1 and 2 (red dashed line). A good estimation of the experiments was observed when the substrate is heated, and the deviation was less than 7%. However, at ambient temperature, this model overestimated the evaporation rate by 20%.

It is worth mentioning that the developed model is close to the one proposed by Kelly-Zion *et al.*²² at ambient temperature and tested on droplets of various sizes and various liquid volatilities (3MP, hexane, cyclohexane, and heptane). The values obtained for the coefficient a and the exponent b of the convective contribution are slightly different, where in their situation, a and b were equal to 0.310 and 0.216, respectively, i.e., relative deviations of 7% for a and 14% for b . Although they observed a good agreement with their investigated fluids, their model also overestimates our data at ambient temperature. In their study, the authors already mentioned the necessity to refine their model for small droplets at ambient temperature.

In summary, the contribution of the atmospheric convective transport has been investigated during the evaporation of a sessile ethanol droplet. Although a deviation was observed between the experiments and the isothermal diffusion-driven model in usual gravity conditions “1 g”, a good agreement was observed in the absence of gravity “ μg ”, regardless of the substrate temperature. These results validated the assumptions inherent in the model in “ μg ” and consequently highlighted the fact that the underprediction of this model is due to the contribution of the buoyant convection in the gas phase, which develops under the action of gravity and was not taken into account. The study of the origin of the convective transport revealed that the solutal aspect was dominant, and a combined diffusive and naturally convective vapor

transport model was proposed. This extended model shows a good agreement with the experimental data whatever the temperature of the substrate, except at ambient temperature, where the model may require a refinement.

The authors acknowledge the financial support of the “Centre National d’Études Spatiales” and also for the parabolic flights conducted at Bordeaux Merignac, France. We also thank Novespace for their assistance during the flights, Pierre Lantoine and Antoine Diana for their friendly technical support.

¹R. Picknett and R. Bexon, *J. Colloid Interface Sci.* **61**, 336–350 (1977).

²H. Hu and R. G. Larson, *J. Phys. Chem. B* **106**, 1334–1344 (2002).

³R. Deegan, O. Bakajin, T. Dupont, G. Huber, S. Nagel, and T. Witten, *Phys. Rev. E* **62**, 756 (2000).

⁴L. V. Govor, G. Reiter, G. H. Bauer, and J. Parisi, *Appl. Phys. Lett.* **84**, 4774 (2004).

⁵V. H. Chhasatia, A. S. Joshi, and Y. Sun, *Appl. Phys. Lett.* **97**, 231909–231909-3 (2010).

⁶L. Pauchard, F. Parisse, and C. Allain, *Phys. Rev. E* **59**, 3737 (1999).

⁷H. Y. Erbil and R. A. Meric, *J. Phys. Chem. B* **101**, 6867–6873 (1997).

⁸K. Lee, C. Cheah, R. Copleston, V. Starov, and K. Sefiane, *Colloids Surf. A* **323**, 63–72 (2008).

⁹H. Gelderblom, A. G. Marin, H. Nair, A. van Houselt, L. Lefferts, J. Snoeijer, and D. Lohse, *Phys. Rev. E* **83**, 026306 (2011).

¹⁰B. Sobac and D. Brutin, *Langmuir* **27**, 14999–15007 (2011).

¹¹S. David, K. Sefiane, and L. Tadrict, *Colloids Surf. A* **298**, 108–114 (2007).

¹²W. Ristenpart, P. Kim, C. Domingues, J. Wan, and H. Stone, *Phys. Rev. Lett.* **99**, 234502 (2007).

¹³K. Sefiane and R. Bennacer, *J. Fluid Mech.* **667**, 260–271 (2011).

¹⁴B. Sobac and D. Brutin, *Phys. Rev. E* **86**, 021602 (2012).

¹⁵F. Girard and M. Antoni, *Langmuir* **24**, 11342–11345 (2008).

¹⁶M. A. Saada, S. Chikh, and L. Tadrict, *Phys. Fluids* **22**, 112115 (2010).

¹⁷L. Bin, R. Bennacer, and A. Bouvet, *Appl. Therm. Eng.* **31**, 3792–3798 (2011).

¹⁸F. Girard, M. Antoni, S. Faure, and A. Steinchen, *Colloids Surf., A* **323**, 36–49 (2008).

¹⁹Y. O. Popov, *Phys. Rev. E* **71**, 036313 (2005).

²⁰F. Carle, B. Sobac, and D. Brutin, *J. Fluid Mech.* **712**, 614–623 (2012).

²¹D. Green and R. Perry, *Perry’s Chemical Engineers’ Handbook*, 8th ed. (McGraw-Hill Professional, 2007).

²²P. Kelly-Zion, C. Pursell, S. Vaidya, and J. Batra, *Colloids Surf., A* **381**, 31–36 (2011).